A Generalized Modeling of a PV System using Matlab Simulation with MPPT for the Speed Control of a 3-Phase Induction Motor

Hitesh Joshi, Poonam Lodhi, Pankaj Kumar

Abstract— In this paper the speed control of three-phase induction motor is achieved and also the analysis of the motor parameters have been done with the help of the modeling and simulation of the induction motor in MATLAB 2011b. The photovoltaic (PV) array is used as a source which is taking the solar irradiation in the input, through which the induction motor is being operated. The PV array is modeled by connecting various solar cells in series and parallel combinations. The simulation of the PV array is done in the MATLAB 2011b software. The maximum power point tracking (MPPT) method is used to track the maximum possible power, and is modeled using the perturb and observe (P & O) algorithm. The modeling of the dc-dc buck converter is done to step-up the voltage to the desired level .To transform the dc voltage into the ac voltage an inverter is employed , which is getting the gate pulses from the pulse width modulation (PWM) generator. The PWM generator is generating the signals from the control strategy being used to convert the voltage from the two-axis reference frame to the three- phase and vice-versa. The modeling and simulation of each part is performed individually.

Index Terms— dc-dc converter, MATLAB, MPPT, PVarray, P & O, PWM, two-axis reference frame.

1 INTRODUCTION

The international agendas of Global warming and Green house gases had drawn affective concerns on the energy policies of the all countries in the world. Developed countries are trying to sort out the problems of excessive emissions of the green house gases. Other major concerns in the power sector developing due to today's scenario is the unavailability to achieve power demand using conventional sources of energy. In fact the continuous use of fossil fuels to meet the required demand has subsequently caused in the reduction of fossil fuel deposit and had also affected the environment drastically depleting the biosphere and cumulatively adding to global warming. In this context, the need for other forms of energy sources to tackle these above mentioned problems are required in a more challenging manner.

- **Hitesh Joshi** is currently pursuing masters degree program in electrical power systems in Suresh Gyan Vihar University, Jaipur, PH-90241588398. E-mail: haitijoshi@gmail.com
- **Poonam Lodhi** is currently pursuing masters degree program in electrical power systems in Suresh Gyan Vihar University, Jaipur, PH-8302214291. E-mail: lodhi.poonam18@gmail.com
- Pankaj Kumar is currently working at as Asstt. Professor & Scientist at Centre of Excellence, Solar Energy Research & Utilization, Suresh Gyan Vihar University, Jaipur, PH-9896998967. E-mail: rudrraa777@gmail.com

One of the best alternatives in this regard is the use of renewable sources of energy which has grown rapidly in recent years. The increasing interest which is building up for the efficient use of renewable energies is due to the fact that the energy policies in the world are trying to fight against the emissions of CO_2. One of the most promising and largely available renewable energy sources is the solar energy.

The basic aim behind the paper is to carry out the modeling and simulation of the photovoltaic array, which is utilizing one of the form of the renewable source of energy, i.e. the solar energy. The PV array is constructed by connecting several solar cells in series and parallel combination. The three-phase induction motor which is connected as a load is then driven by the PV array. The main aim to operate the induction motor is due to the wide range of industrial applications associated with this motor and the continous operation of the motor from the past few decades.

2 Modeling of Photovoltaic Panel

Photovoltaic (PV) or solar cells as they are also called semiconductor devices because they convert sunlight into direct current (DC) or electricity. Groups of PV cells are electrically configured into modules and arrays, which can be

used to charge batteries, operate motors, and to power any number of electrical loads. By using the appropriate power conversion equipment, PV systems can produce alternating current (AC) compatible with any conventional appliances, and can operate in parallel with, and interconnected to, the utility grid.

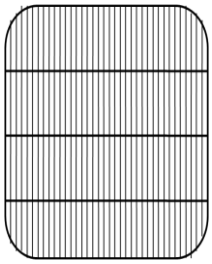

Fig. 1: PV Cell

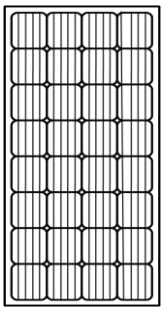

Fig. 2: PV Module

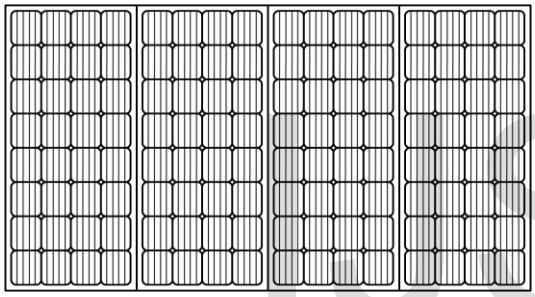

Fig. 3: PV Array

The equivalent circuit of the PV cell is shown in Figure 1. PV cells are grouped in larger units called PV panels which are further interconnected in a parallel-series configuration to form PV arrays.To simulate the array, cell model parameters are properly multiplied by number of cells.

The model equations are given from

$$I_D = I_O * (e^{\frac{V_{C*}q}{ak\,Tck}} - 1) \ldots\ldots\ldots\ldots\ldots\ldots\ldots\ldots(1)$$

$$I = I_L - I_O\left(e^{\frac{(V+IR_S)q}{q_k\,T_{ck}}}\right) \ldots\ldots\ldots\ldots\ldots\ldots\ldots\ldots(2)$$

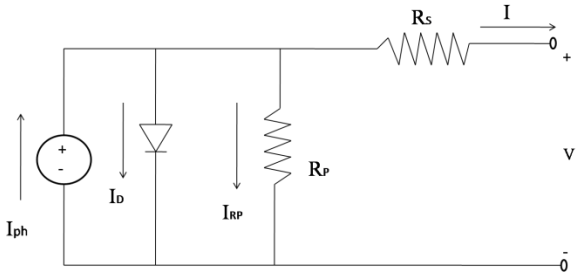

Fig. 4: Simulink model of a PV celL

- **Short Circuit Condition**

According to the short circuit situation in equivalent circuit shown in Fig 4.5, the current relationship can be expressed as

$$I_{ph}\left(G_a, T\right) = I_{scs}\frac{G_a}{G_{as}}[1 + \Delta I_{sc}(T - T_s)] \ldots\ldots(3)$$

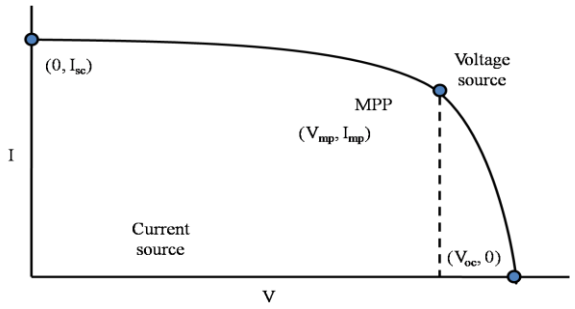

Fig. 5: Characteristic I–V curve of a practical PV device and the three remarkable
points: short circuit (0, Isc), MPP (Vmp, Imp), and open circuit (Voc , 0).

- **Open Circuit Condition**

The open-circuit voltage can be computed as

$$V_{oc}(T) = V_{ocs} + \Delta V_{oc}(T - T_s) \ldots\ldots\ldots\ldots\ldots(4)$$

- **At the peak power point**

The peak power point (V_{mpp} , I_{mpp}) under different testing environment can be known according to the photovoltaic panel's specification. At the peak power point,

$$I_{mpp} = I_{ph} - \left[\frac{e^{\left(\frac{Vmpp+IR_S}{V_t}\right)}-1}{e^{\left(\frac{Voc}{V_t}\right)}-1}\right] I_{ph} \ldots\ldots\ldots\ldots\ldots..(5)$$

The basic equation (5) of the elementary PV cell does not represent the *I–V* characteristic of a practical PV array.

3 Modeling of Induction Motor

The control and speed sensorless estimation of IM drives is a vast subject. Traditionally, the IM has been used with constant frequency sources and normally the squirrel-cage machine is utilized in many industrial applications, A typical construction of a squirrel cage IM is illustrated in Figure 6. Its main advantages are the mechanical and electrical simplicity and ruggedness, the lack of rotating contacts (brushes) and its capability to produce torque over the entire speed range.

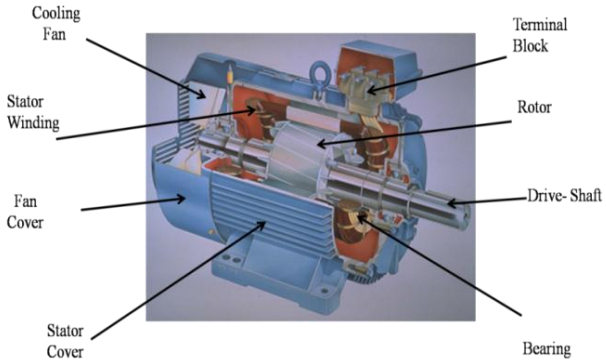

Fig. 6: A cut-away view of a Squirrel Cage Induction Motor

Before going to analyze any motor or generator it is very much important to obtain the machine in terms of its equivalent mathematical equations. Traditional per phase equivalent circuit has been widely used in steady state analysis and design of induction motor, but it is not appreciated to predict the dynamic performance of the motor. The dynamics consider the instantaneous effects of varying voltage/currents, stator frequency, and torque disturbance. The dynamic model of the induction motor is derived by using a two-phase motor in direct and quadrature axes. This approach is desirable because of the conceptual simplicity obtained with two sets of windings, one on the stator and the other in the rotor. The equivalence between the three phase and two phase machine models is derived from simple observation, and this approach is suitable for extending it to model an n-phase machine by means of a two phase machine.

3.1 Reference Frames

The required transformation in voltages, currents, or flux linkages is derived in a generalized way. The reference frames are chosen to be arbitrary and particular cases, such as stationary, rotor and synchronous reference frames are simple instances of the general case. R.H. Park, in the 1920s, proposed a new theory of electrical machine analysis to represent the machine in d – q model. He transformed the stator variables to a synchronously rotating reference frame fixed in the rotor, which is called Park's transformation. He showed that all the time varying inductances that occur due to an electric circuit in relative motion and electric circuits with varying magnetic reluctances could be eliminated.

The voltages v_{ds} and v_{qs} can be resolved into as bs-cs components and can be represented in matrix from as

$$\begin{bmatrix} v_{as} \\ v_{bs} \\ v_{cs} \end{bmatrix} = \begin{bmatrix} \cos\theta & \sin\theta & 1 \\ \cos(\theta - 120^0) & \sin(\theta - 120^0) & 1 \\ \cos(\theta + 120^0) & \sin(\theta + 120^0) & 1 \end{bmatrix} \begin{bmatrix} v_{qs} \\ v_{ds} \\ v_{0s} \end{bmatrix}$$

……..…….(6)

Here v_{0s} is zero-sequence component, convenient to set $\Theta = 0$ so that qs axis is aligned with as-axis. Therefore ignoring zero-sequence component, it can be simplified as

$$v_{qs} = \frac{2}{3} v_{as} - \frac{1}{3} v_{bs} - \frac{1}{3} v_{cs} \qquad \text{…….(7)}$$

$$v_{ds} = -\frac{1}{\sqrt{3}} v_{bs} - \frac{1}{\sqrt{3}} v_{cs} \qquad \text{……(8)}$$

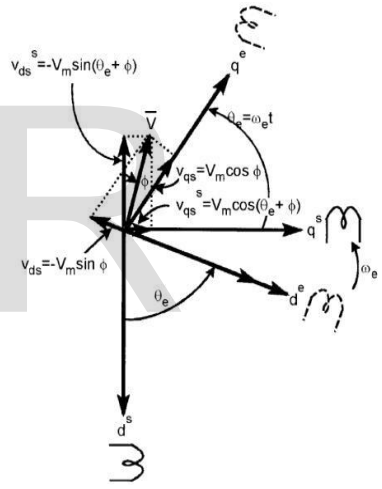

Fig. 7: stationary frame d^s-q^s to dynchronously rotating frame d^e-q^e transformation

Equations (7) and (8) consistively called as Clark Transformation. Figure (7) shows the synchronously rotating d^e-q^e axes, which rotate at synchronous speed we with respect to the d^s-q^s axes and the angle $\theta_y = \omega_e *$. The two-phase d^s-q^s windings are transformed into the hypothetical windings mounted on the d^e-q^e axes. The voltages on the d^s-q^s axes can be transformed (or resolved) into the d^e-q^e frame as per the equations.

3.2 Dynamic equations of Induction Machine

Generally, an IM can be described uniquely in arbitrary rotating frame, stationary reference frame or synchronously

rotating frame. For transient studies of adjustable speed drives, it is usually more convenient to simulate an IM and its converter on a stationary reference frame. Moreover, calculations with stationary reference frame are less complex due to zero frame speed. For small signal stability analysis about some operating condition, a synchronously rotating frame which yields steady values of steady-state voltages and currents under balanced conditions is used.

From the above figure the terminal voltages are as follows,

$$v_{qs} = R_q i_{qs} + p(L_{qq} i_{qs}) + p(L_{qd} i_{ds}) + p(L_{q\alpha} i_{\alpha}) + p(L_{q\beta} i_{\beta}) \quad \ldots\ldots\ldots\ldots\ldots\ldots(8)$$

$$v_{ds} = p(L_{dq} i_{qs}) + R_d i_{ds} + p(L_{dd} i_{ds}) + p(L_{d\alpha} i_{\alpha}) + p(L_{d\beta} i_{\beta}) \quad \ldots\ldots\ldots\ldots\ldots\ldots(9)$$

$$v_{\alpha} = p(L_{\alpha q} i_{qs}) + p(L_{\alpha d} i_{ds}) + R_{\alpha} i_{\alpha} + p(L_{\alpha\alpha} i_{\alpha}) + p(L_{\alpha\beta} i_{\beta}) \quad \ldots\ldots\ldots\ldots\ldots\ldots(10)$$

$$v_{\beta} = p(L_{\beta q} i_{qs}) + p(L_{\beta d} i_{ds}) + p(L_{\beta\alpha} i_{\alpha}) + R_{\beta} i_{\beta} + p(L_{\beta\beta} i_{\beta}) \quad \ldots\ldots\ldots\ldots\ldots\ldots..(11)$$

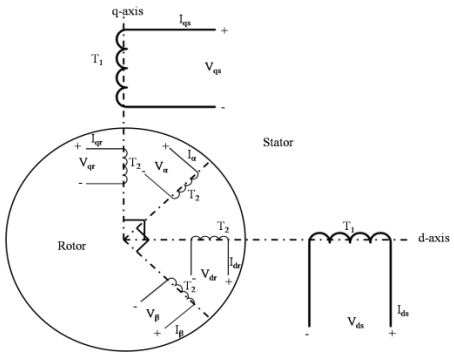

Fig. 8: Two-phase equivalent diagram of induction motor

Where,

p = differential operator $\frac{d}{dt}$

v_{qs}, v_{ds} = terminal voltages of the stator q and d axis

v_{α}, v_{β} = voltages of rotor α and β windings

i_{qs}, i_{ds} = stator q and d axis currents

i_{α}, i_{β} = rotor α and β winding current

L_{qq}, L_{dd} = the stator q and d axis winding self inductances

$L_{\alpha\alpha}, L_{\beta\beta}$ = rotor α and β winding self-inductances

The following are the assumptions made in order to simplify the equation

i. Uniform air-gap

ii. Balanced rotor and stator windings with sinusoidally distributed mmfs

iii. Inductance in rotor position is sinusoidal and

iv. Saturation and parameter changes are neglected

The rotor equations in above equation (7) and (8) are refereed to stator side as in the case of transformer equivalent circuit. From this, the physical isolation between stator and rotor d-q axis is eliminated.

dynamic equations of the induction motor in any reference frame can be represented by using flux linkages as variables. This involves the reduction of a number of variables in the dynamic equations.

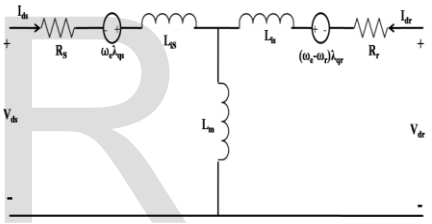

Fig. 9: d-axis equivalent circuit

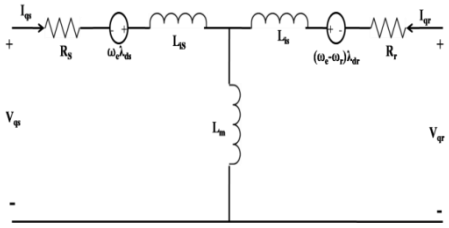

Fig. 10: q-axis equivalent circuit

Even when the voltages and currents are discontinuous the flux linkages are continuous. The stator and rotor flux linkages in the stator reference frame are defined as

$$\psi_{qs} = L_s i_{qs} + L_m i_{qr} \quad \ldots\ldots\ldots\ldots(12)$$

$$\psi_{ds} = L_s i_{ds} + L_m i_{dr} \quad \ldots\ldots\ldots\ldots..(13)$$

$$\psi_{qr} = L_r i_{qr} + L_m i_{qs} \quad \ldots\ldots\ldots\ldots..(14)$$

$$\psi_{dr} = L_r i_{dr} + L_m i_{ds} \quad \ldots\ldots\ldots\ldots(15)$$

$$\psi_{qm} = L_m(i_{qs}+i_{qr}) \quad \text{……(16)}$$

$$\psi_{dm} = L_m(i_{ds} + i_{dr}) \text{……..(17)}$$

From (12) to (17) we get

$$v_{ds} = R_s i_{ds} + p\psi_{ds} \text{……..(18)}$$

$$v_{qs} = R_s i_{qs} + p\psi_{qs} \quad \text{……. …….(19)}$$

$$v_{dr} = R_r i_{dr} + \omega_r \psi_{dr} + p\psi_{dr} \text{ ……..(20)}$$

$$v_{qr} = R_r i_{qr} - \omega_r \psi_{qr} + p\psi_{qr} \text{……..(21)}$$

Since the rotor windings are short circuited, the rotor voltages are zero. Therefore

$$R_r i_{dr} + \omega_r \psi_{dr} + p\psi_{dr} = 0 \quad \text{…….(22)}$$

$$R_r i_{qr} - \omega_r \psi_{qr} + p\psi_{qr} = 0 \quad \text{……. (23)}$$

From equation (22) and (23) we get

$$i_{dr} = \frac{-\omega_r \psi_{dr} - p\psi_{dr}}{R_r} \quad \text{……..(24)}$$

$$i_{qr} = \frac{\omega_r \psi_{qr} - p\psi_{qr}}{R_r} \quad \text{……..(25)}$$

By solving the equations (18), (19),(20) and (21) we get the following equations

$$\psi_{ds} = \int (v_{ds} - R_s i_{ds}) dt \quad \text{……(26)}$$

$$\psi_{qs} = \int (v_{qs} - R_s i_{qs}) dt \quad \text{……(27)}$$

$$\psi_{dr} = \frac{-L_r \omega_r \psi_{qr} + L_m i_{ds} R_r}{R_r + sL_r} \quad \text{……(28)}$$

$$\psi_{qr} = \frac{L_r \omega_r \psi_{dr} + L_m i_{qs} R_r}{R_r + sL_r} \quad \text{……..(29)}$$

$$i_{ds} = \frac{v_{ds}}{R_s + sL_s} - \left[\frac{\psi_{dr} sL_m}{L_r(R_s + sL_s)}\right] \quad \text{……(30)}$$

$$i_{qs} = \frac{v_{qs}}{R_s + sL_s} - \left[\frac{\psi_{qr} sL_m}{L_r(R_s + sL_s)}\right] \quad \text{……(31)}$$

The electromagnetic torque of the induction motor in stator reference frame is given by

$$T_e = \frac{3}{2}\frac{p}{2} L_m(i_{qs} i_{dr} - i_{ds} i_{qr}) \quad \text{……(32)}$$

or

$$T_e = \frac{3}{2}\frac{p}{2}\frac{L_m}{L_r}(i_{qs}\psi_{dr} - i_{ds}\lambda_{qr}) \quad \text{……(33)}$$

For positive values of slip, the torque-speed curve has a peak. This is the maximum torque produced by the motor and is called the breakdown torque or the stalling torque. Its value can be calculated by differentiating the torque expression with respect to slip and then setting it to zero to get ŝ, the slip at the maximum torque.

Slip at maximum torque

$$s = \pm \frac{R_r'}{\sqrt{R_r'^2 + (X_{1s} + X_{1r}')^2}} \quad \text{……(34)}$$

Maximum torque,

$$T_{emax} = \frac{3v_s^2}{2\omega_s} \cdot \frac{1}{R_s \pm \sqrt{R_r'^2 + (X_{1s} + X_{1r}')^2}} \quad \text{……(35)}$$

From equation (35) we observe that the torque is proportional to the square of applied voltage.

To avoid saturation in the motor, the air-gap flux must be kept constant. The developed torque is given as

$$T_{E/f} = \frac{K^2 f^2}{\left(\frac{R_r'}{s}\right)^2 + (\omega L_{1r}')^2} \cdot \frac{R_r'}{s\omega} \quad \text{……(36)}$$

Slip at maximum torque,

$$s_{max} = \pm \frac{R_r'}{\omega L_r'} \quad \text{……..(37)}$$

Maximum torque,

$$T_{E/f} = \frac{K_2}{8\pi^2 L_{1r}} \quad \text{……..(38)}$$

Equation (38) shows that the maximum torque is independent of frequency and hence remains the same for each E/f and the maximum torque occurs at a speed [26] lower than the synchronous speed for each combination of E and f . However, we get a slightly different set of curves for constant V/f, so for fixed V, E changes with operating slip and the maximum torque is reduced.

4 SIMULATION AND RESULTS

4.1 Simulation Model of the System

The Simulink model of the PV system used for the implementation in driving the three-phase induction motor, alongwith the boost converter and inverter is shown fig 11.

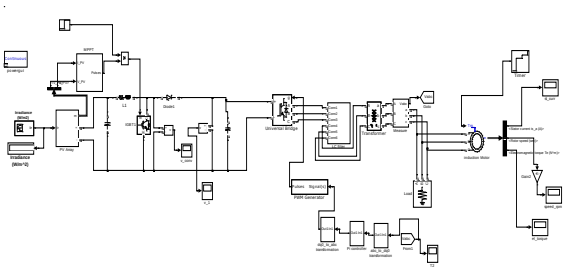

Fig. 11: Simulation model of the overall proposed work

In this Simulation model, a PV array is chosen and given the variable irradiance in terms of constant, step and ramp inputs. The maximum power of this PV array is taken using the MPPT which is developed using the P & O algorithm. The various other elements which are used to construct this model include the boost converter, which is used to step up the voltage to the required value. The IGBT based inverter is used to convert the dc voltage into the ac voltage and the input to this inverter is provided using the PWM generator, in which the signals are generating from the control circuit. The inverter is then connected to the L-C filter to eliminate the harmonics of the ac voltage. A three-phase step-down transformer is used to decrease the voltage up to the required limits for driving a three-phase parallel RLC load attached to the system, and basically to provide the sufficient voltage to drive the three-phase induction motor load.

4.2 PV Module Simulation

The PV cell is constructed using the single diode model. The I_{ph} which is given in the input of the cell model is basically the photo-generated current. This consists of a R_s resistor in series and R_p resistor in parallel. This was modeled using the Sim Power system block in the MATLAB library.The simulation model is shown below.

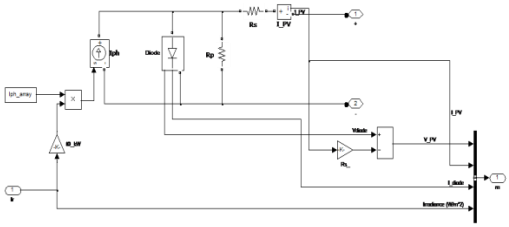

Fig. 12: Simulation model of a PV Array

A controlled current source is been used to drive the solar cell. The PV array is then constructed using various number of solar cells connected in series and in parallel. The input to this array is provided for different solar irradiations.

C. Solar Cell with MPPT

The current and voltage of the PV array is given out to the MPPT block, which determines the maximum power output of the model. The point at which the maximum power is obtained is tracked by using the P & O method. An algorithm based analysis is done for this purpose which utilizes the power and voltage values being measured at different time intervals and a comparison based study is carried out to locate the MPP.

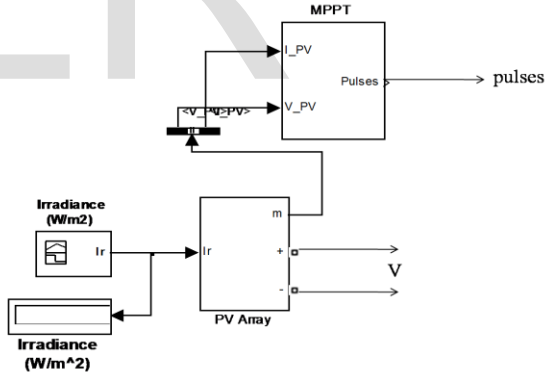

Fig. 13: Simulation model of the MPPT

The unit in which the gating signal is provided uses the MPPT algorithm of the P & O method where the change in power, change in voltage, instantaneous power and instantaneous current values are taken into account to do the necessary duty cycle variations. The repeating sequence being utilized in the model has an operating frequency of f KHz. This is also the frequency of the gating signal.

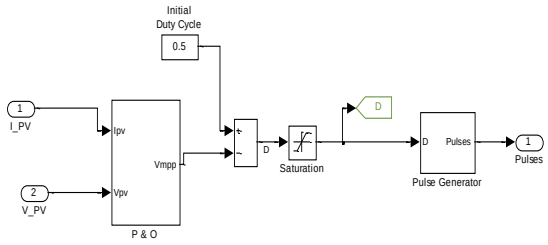

Fig 14: Modeling of P&O Algorithm

4.3 DC-DC Converter Circuit

The dc-dc boost converter is utilized to step up the voltage to the specified level and it consists of a L mH inductor with a R_s ohm resistor and a C µF capacitor. The gating signal to the boost converter is generated by comparing the signal generated by the MPPT algorithm to a repeating sequence operating at a high frequency.

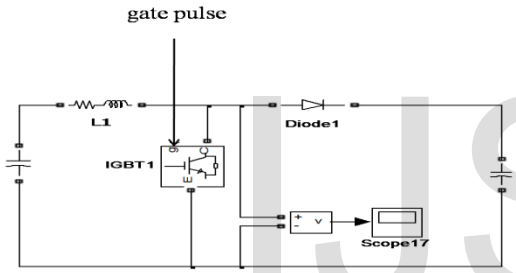

Fig 15: Simulation Model of Boost Converter

4.4 Inverter Circuit

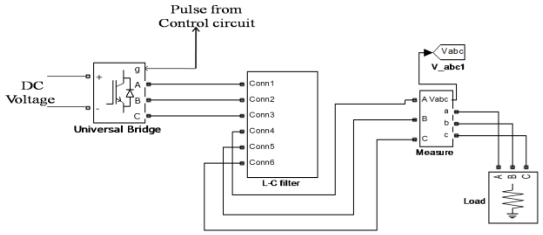

Fig. 16: Simulation model of Inverter circuit

The dc voltage which is coming from the dc-dc converter is converted to the ac voltage using the IGBT based inverter, which is modeled using the blocks provided in the library icon of MATLAB. The gating signal to this inverter is provided from the control circuitry which is explained later.

4.5 Control Circuit

The three-phase ac voltage which is obtained after the overall simulation and measured by the three-phase measurement block of the simulink library is given in the input of the three-phase PLL block, which tracks the frequency and phase of a sinusoidal three-phase signal by using an internal frequency oscillator, which helps to keep the phase difference to zero.

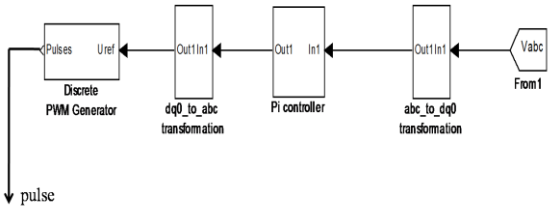

Fig. 16: Simulation model of the Control Circuit

The three-phase sinusoidal voltage obtained from the PLL block is then applied to the abc to dq0 transformation block, which computes the direct axis, quadratic axis, and zero sequence quantities in a two-axis rotating reference frame for a three-phase sinusoidal signal. The two-axis transformed voltage is compared with the reference values of the direct axis and quadrature axis and through the selector are given to the PI controller block, which uses the gains to tune the response time, overshoot, and steady-state error performances. The voltage from this block is further applied to the inverse Park transformation block, which change the two-axis rotating reference frame voltages back to the three-phase voltages. These voltages are then given to the PWM pulse generator having a carrier frequency of f KHz, and the signals provided from this generator are applied to the inverter.

4.6 Induction Motor

A 3 HP squirrel cage induction motor is used to carry out the performance analysis of various quantities such as the stator current, electromagnetic torque according to the applied system voltage and their parameters are so arranged in relation to this voltage. The speed control of the three-phase induction motor is carried out, while setting the timer for different time amplitudes.

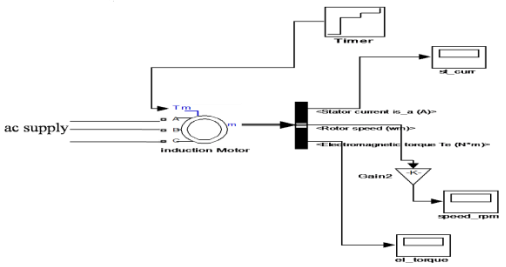

Fig. 17: Induction motor model

4.7 Results

The PV module consists of following parameters:

Number of cells per module = 96

Number of series-connected modules per string = 5

Number of parallel strings = 66.

Irradiance = 1000 W/m^2

The dc voltage which is generated by the PV array is of very low magnitude of 300 V and after boosting it through the dc-dc converter it reaches to a much greater amplitude, i.e. up to 600 V.

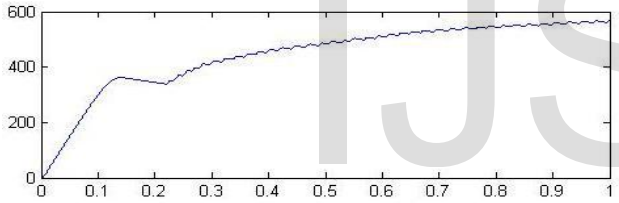

Fig. 18: DC voltage

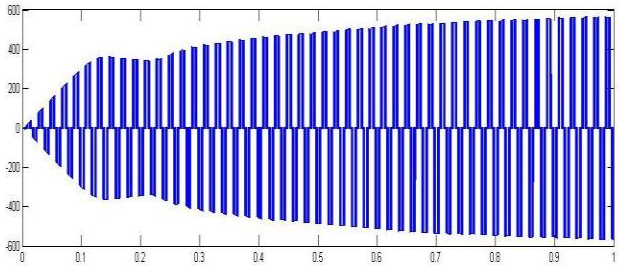

Fig.19: Inverter voltage

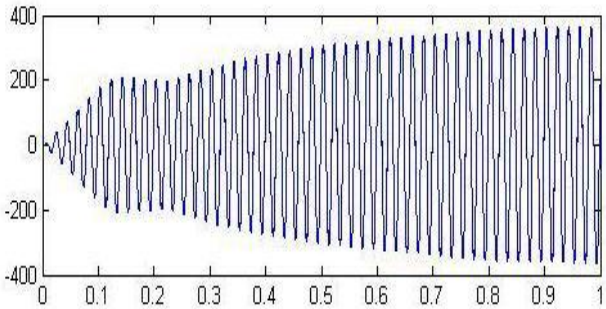

Fig. 20: Load Voltage

The dc voltage after attaining the higher magnitude level while passing it through the boost converter is converted to the ac voltage and the harmonics of this voltage are eliminated with the help of L-C filter, and this voltage is then step-down to 380 V using the transformer, as shown in figure (20).

1) Motor Results

The induction motor chosen for the simulation studies has the following parameters:

Parameter	Value
Supply Voltage	380 V
Frequency	50 Hz
Rotor Type	Squirrel Cage
Motor Rating	2.2 kW (3 HP)
Number of Poles	4
Nominal Speed	1750 rpm

Table 1 Parameters chosen for the simulation

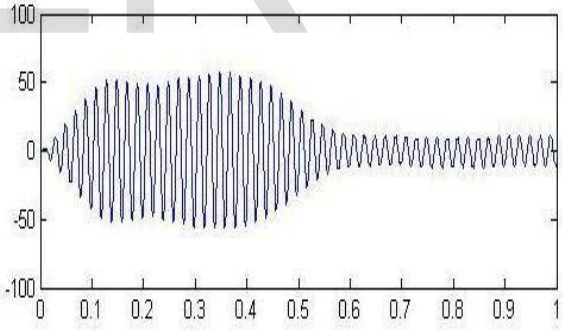

Fig. 21: Stator Current

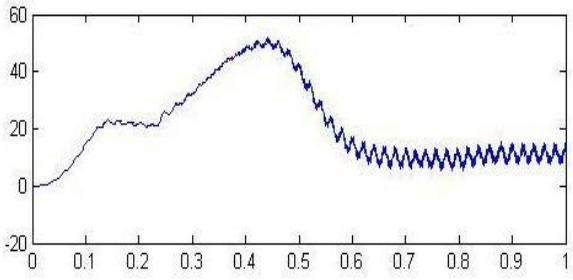

Fig. 22: Load Torque

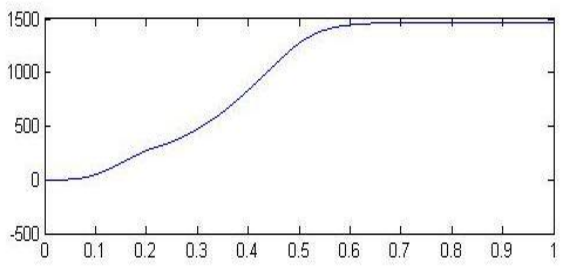

Fig. 23:Speed of the motor

Figure (21) shows the stator current. The stator current is found to be quite noisy and is initially ramping in nature, however these are settled after attaining the peak value at 50 Hz. The same ripples are also introduced in the electromagnetic torque, which is shown in figure (22). The speed of the motor initially operating at 50 Hz has risen from zero and has increased above the nominal speed. The motor speed also experiences some disturbances in the starting but afterwards settled to a steady level just in few milliseconds, which is basically due to the inertia of the motor which is preventing this disturbance to occur in the motor speed waveform, shown in figure (23).

2) FFT Analysis

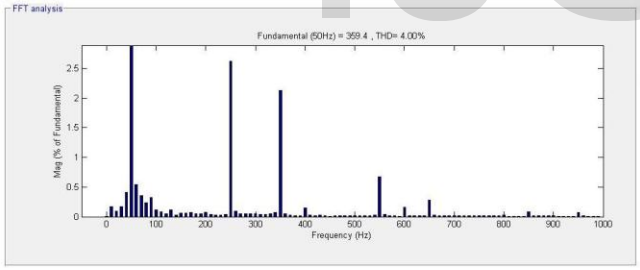

Fig. 24: FFT Analysis

The FFT analysis of the line voltage is shown in figure (24) and total harmonic distortion (THD) gets reduce to 4%, and hence the lower order harmonics are eliminated.

5 CONCLUSION

In this paper, we have studied the speed control of a three-phase Induction Motor and carried out the performance analysis of the motor parameters. The parameters of the motor were obtained according to the specifications and the input been provided to it. The modeling and simulation of the PV array ensures and help us for the use of renewable source of energy for driving the motor, which is the prime requirement of today's and future power sector to implement these sources for the operation of such motors since the induction motors are commonly used in several industrial applications. The advantage of driving the motor with the help of solar energy, which is done in the thesis is that with the variable solar irradiations and the use of MPPT, we have carried out the operation and working of several horse-power rated motor with ease and consequently achieve this by obtaining several advantages such as energy saving, low motor starting current, easy to install and high power factor.

ACKNOWLEDGEMENT

First of all, I would like to Thank my Parents for providing me support and resources, which helped me to complete my paper successfully and also for supporting my interest in this field. Next, I would like to express heartily gratitude to my supervisor, Asstt. Professor of Department of Electrical Engineering, Suresh Gyan Vihar University, Mr.Pankaj Kumar for his valuable technical suggestions and full guidance towards completion of my paper from the beginning till the end.

REFERENCES

[1] Mairaj Aftab Malik, Omar Kiyani, and Arvind Srinivasan, "Alternative Solar Cells and Their Implications", An Interactive Qualifying Project, Worcester Polytechnic Institute, MA, March 2010.

[2] Weidong Xiao, William G. Dunford, and Antoine Capel, "A Novel Modeling Method for Photovoltaic Cells", 35th Annual IEEE Power Electronics Specialists Conference, Germany, pp. 1950-1956, 2004.

[3] M. G. Villalva, J. R. Gazoli, and E. R. Filho, "Comprehensive Approach to Modeling and Simulation of Photovoltaic Arrays", IEEE Trans. Power Electronics, Vol. 24, No.5, pp. 1198-1208, May 2009.

[4] M. Berrera, A. Dolara, R. Faranda and S. Leva, "Experimental test of seven widely-adopted MPPT

algorithms", 2009 IEEE Bucharest Power Tech Conference, June 28th - July 2nd, Bucharest, Romania.

[5] "Modeling simulation and analysis of a permanent magnet brushless dc motor drive," presented at the IEEE IAS Annual Meeting, Atlanta, 1987.

[6] S. Funabiki and T. Himei, "Estimation of torque pulsation due to the behavior of a converter and an inverter in a brushless dc-drive system," Proc. Inst. Elec. Eng., vol. 132, part B, no. 4, pp. 215-222, July 1985.

[7] Scott Wade, Matthew W. Dunnigan, and Barry W. Williams, "Modelling and Simulation of Induction Machine Vector Control with Rotor Resistance Identification", IEEE transactions on power electronics, vol. 12, no. 3, may 1997.

[8] Jotten, R. and Maeder, G. (1983). Control methods for good dynamic performance induction motor drives based on current and voltages as measured quantities. IEEE Transactions on Industrial Applications, vol. IA-19, no. 3: pp. 356-363.

[9] Abbondanti, A. and Brennen, M.B. (1975). Variable speed induction motor drives use electronic slip calculator based on motor voltages and currents. IEEE Transactions on Industrial Applications, vol. IA-11, no. 5: pp. 483-488.

[10] Baader, U., Depenbrock, M. and Gierse, G. (1989). Direct self control of inverter-fed induction machine, a basis for speed control without speed measurement. Proc. IEEE/IAS Annual Meeting, pp. 486-492.

[11] Viorel, I. A. and Hedesiu, H. (1999). On the induction motors speed estimator's robustness against their parameters. IEEE Journal. pp. 931-934.

[12] Adel Aktaibi & Daw Ghanim, and M. A. Rahman, "Dynamic Simulation of a Three-Phase Induction Motor Using Matlab Simulink", IEEE precedings, St. John's, NL, Canada.

[13] Kottala Kiran Kumar, S.Sasikanth and L.Dinesh, " Simulation Of Sensorless Induction Motor Based On Model Reference Adaptive System (MRAS)", IJERA Vol. 2, Issue 6, November- December 2012, pp.255-260.

[14] Jeetesh Kumar, and Kamakhya Prasad Basumatary, "Speed Control of Induction Motor using V/f Technique", A thesis report submitted to IIT Guwahati, 2011.

[15] Aleck W. Leedy, "Simulink / MATLAB Dynamic Induction Motor Model for Use as ATeaching and Research Tool", International Journal of Soft Computing and Engineering (IJSCE) ISSN: 2231-2307, Volume-3, Issue-4, September, 2013.

[16] Enemuoh F. O., Okafor E. E., Onuegbu J. C., and Agu V. N., "Modelling, Simulation and Performance Analysis of A Variable Frequency Drive in Speed Control Of Induction Motor", International Journal of Engineering Inventions e-ISSN: 2278-7461, p-ISSN: 2319-6491, pp. 36-41 Volume 3, Issue 5 (December 2013).

[17] Abhinav, and Venu Sangwan, "Normalized Dynamic Simulation of 3-phase Induction Motor using MATLAB/SIMULINK", International Journal of Emerging Technology and Advanced Engineering, Volume 4, Issue 3, pp. 43-48, March 2014.

[18] Anjana Manuel, Jebin Francis, "Simulation of Direct Torque Controlled Induction Motor Drive by using Space Vector Pulse Width Modulation for Torque Ripple Reduction", IJAREEIE, Vol. 2, Issue 9, September 2013.